

Short-Range Excitonic Phenomena in Low-Density Metals

Jaakko Koskelo,^{1,2} Lucia Reining^{1,2}, and Matteo Gatti^{1,2,3}

¹*LSI, CNRS, CEA/DRF/IRAMIS, École Polytechnique, Institut Polytechnique de Paris, F-91120 Palaiseau, France*

²*European Theoretical Spectroscopy Facility (ETSF)*

³*Synchrotron SOLEIL, L'Orme des Merisiers, Saint-Aubin, BP 48, F-91192 Gif-sur-Yvette, France*



(Received 7 December 2022; accepted 16 December 2024; published 27 January 2025)

Excitonic effects in metals are usually supposed to be weak, because the Coulomb interaction is strongly screened. Here, we investigate the low-density regime of the homogeneous electron gas, where, besides the usual high-energy plasmons, the existence of low-energy excitonic collective modes has recently been suggested. Using the Bethe-Salpeter equation (BSE), we show that indeed low-energy modes appear, thanks to reduced screening at short distances. This requires going beyond common approximations to *ab initio* BSE calculations, which suffer from a self-polarization error that overscreens the electron-hole interaction. The electron-hole wave function of the low-energy mode shows strong and very anisotropic electron-hole correlation, which speaks for an excitonic character of this mode. The fact that the electron-hole interaction at short distances is at the origin of these phenomena explains why, on the other hand, also the simple adiabatic local density approximation to time-dependent density functional theory can capture these effects. This exotic regime might be found in doped semiconductors and interfaces.

DOI: [10.1103/PhysRevLett.134.046402](https://doi.org/10.1103/PhysRevLett.134.046402)

Excitons, pairs of an electron and a hole that interact via the screened Coulomb interaction, often dominate the low-energy range of absorption spectra in insulators or low-dimensional materials, where the dielectric screening is weak [1–3]. Excitons play a crucial role as energy carriers in many optoelectronic devices, such as solar cells, light-emitting diodes, single-photon emitters, etc. In metals, instead, which behave approximately like a homogeneous electron gas (HEG), the dominant excitations are plasmons, collective oscillations at higher frequencies, which originate from coupling of density changes by the long-range bare Coulomb interaction. They are well captured by the random-phase approximation (RPA) [4,5], where the electron-hole (*e-h*) interaction is neglected.

However, quantum Monte Carlo (QMC) simulations for the many-body ground state predict a complex phase diagram for the HEG [6–12]. In particular, for a Wigner-Seitz radius $r_s > 5.25$, negative static screening is found [13], which is related to imaginary poles in the dielectric function that were originally called ghost plasmons [15,16]. Recently, using advanced approximations of time-dependent density functional theory (TDDFT), Takada [17,18] predicted poles in the inverse dielectric function of excitonic, rather than plasmonic, character. Their fingerprint should be a collective mode in the dynamic structure factor at small energies ω and large wave vectors q , which might be detected by inelastic x-ray scattering or electron energy loss spectroscopy [19]. Time-resolved experiments have identified transient excitons at metal surfaces [20]. Still, the impact of excitonic

effects for valence electrons of metals remains largely unexplored and their existence to be confirmed [21].

The propagation of interacting electrons and holes is described by the Bethe-Salpeter equation (BSE) [3,22,23] of many-body-perturbation theory. In the time-dependent screened Hartree-Fock approximation electrons and holes interact with each other through a screened Coulomb potential. When the full microscopic screening is replaced by the macroscopic dielectric constant, the widely used Wannier-Mott exciton model can be derived [1–3]. In metals like the HEG, Wannier-Mott excitons should not form because the macroscopic screening by free carriers is perfect [11,24–26]. If excitons exist in the HEG, they must be allowed by phenomena that go beyond such models. Macroscopic screening is a strong oversimplification: only at very large distances an added charge and its screening cloud act like a single, reduced effective charge, which amounts to zero in a metal. At shorter distances, microscopic details of the screening cloud, and its spatial extension, become important. Close to the added charge, the full bare Coulomb potential is felt, and the effect of the screening cloud becomes negligible. Therefore, at short distances an electron and a hole can attract each other, even in metals.

To the best of our knowledge, the first-principles BSE, which takes into account the full microscopic screening, has never been solved in low-density metals or HEG. Our work bridges this gap, aiming to elucidate whether the BSE finds ghost modes and low-energy collective modes at low densities. If so, we can address three challenging questions:

Are these modes indeed of excitonic character? Which are the key ingredients that allow them to develop in a metal? And therefore, how can we predict them, and in which realistic situation could one find them?

In the first principles BSE [3,22,23], the propagation of electrons and holes is governed by a self-energy Σ , and their effective interaction stems from the variation of Σ with respect to the one-body Green's function G . Most often, Σ is used in the GW approximation [27], where the effective electron-electron (e - e) repulsion and electron-hole attraction (e - h) are given by the screened Coulomb interaction $\pm W(q, \omega) = \pm \epsilon^{-1}(q, \omega) v_c(q)$, where the bare Coulomb interaction v_c is screened by the inverse dielectric function ϵ^{-1} . Additionally, a quasiparticle approximation is made for G , and the e - h attraction is taken in its static limit $\omega = 0$. Here, the Tamm-Dancoff approximation is avoided, since the coupling between resonant and antiresonant transitions strongly influences the collective modes (see the Supplemental Material [28]). From the solution of this BSE, called GW-BSE in the following, the microscopic dielectric function $\epsilon(q, \omega)$ is obtained. Since ϵ is also used in input, the formalism is in principle self-consistent, and in practice truncated as summarized in scheme (1):

$$\left. \begin{array}{l} \epsilon^{\text{in}}(q) \rightarrow \Sigma = iGW^{\text{in}}: e\text{-}e \text{ repulsion} \\ \epsilon^{\text{in}}(q) \rightarrow -W^{\text{in}}: e\text{-}h \text{ attraction} \end{array} \right\} \xrightarrow{\text{BSE}} \epsilon^{\text{out}}(q, \omega). \quad (1)$$

Here, $\epsilon^{\text{in}}(q)$ is an approximate dielectric function taken at $\omega = 0$ in both e - e and e - h interactions for consistency [28]. This static approximation to GW gives the COHSEX self-energy. In a metal $1/\epsilon^{\text{in}}(q \rightarrow 0) = 0$ [11,25,26] suggests vanishing excitonic effects. However, little definite knowledge exists, as few BSE calculations in metals can be found, besides work on optical properties [46,47], including low-dimensional materials [48,49], or the correlation energy [50]. In particular, the impact of the momentum dependence of $1/\epsilon^{\text{in}}(q)$ remains to be explored.

Figure 1 shows, as a function of distance r (upper panel) and of wave vector q (bottom panel), the screened Coulomb attraction $-W^{\text{in}}$ in the HEG at $r_s = 22$ obtained from the numerically exact dielectric function extracted from QMC results [29,30] (for smaller r_s see Ref. [28]). This interaction $-W_{\text{QMC}}(r)$ decays rapidly with distance, but it is oscillating and even repulsive for $0.4/k_F < r < 2/k_F$. At short distances $r < 0.4/k_F$ it is strongly attractive. Also in the commonly used RPA [51,52], for $r < 1/k_F$ strong attraction is found for $-W_{\text{RPA}}(r)$. As a consequence, even the standard GW_{RPA} -BSE could, in principle, yield excitons.

We therefore follow scheme (1) using in input $1/\epsilon^{\text{in}}(q) = 1 + v_c(q)\chi(q, \omega = 0)$ with the RPA density-density response function $\chi = \chi_{\text{RPA}}$. In the output $\epsilon^{\text{out}}(q, \omega)$, we search for collective modes with frequency $\omega_c(q)$ defined by $\text{Re } \epsilon^{\text{out}}(q, \omega_c(q)) = 0$. Figure 2 displays the GW_{RPA} -BSE result for $r_s = 22$ (for smaller r_s see Ref. [28]). At low q , we

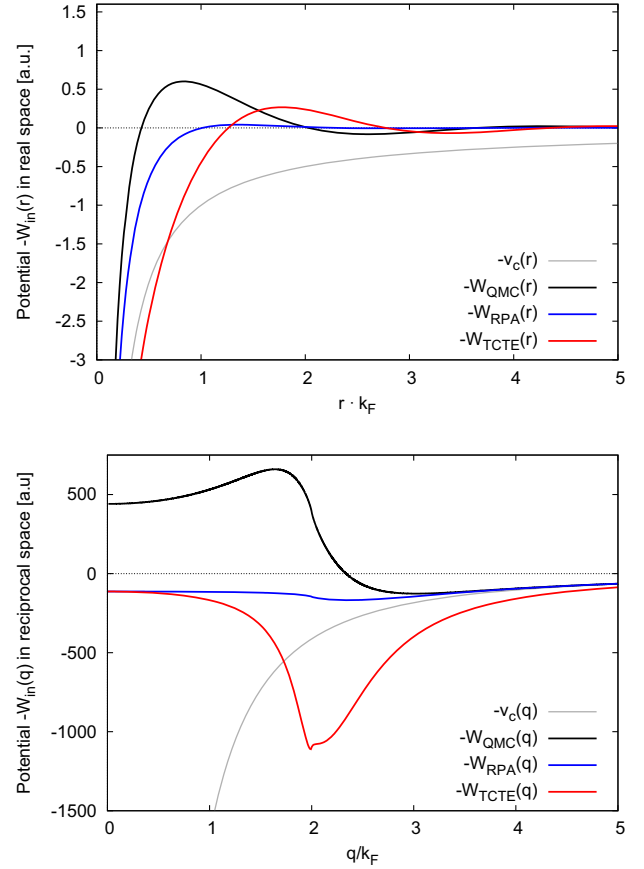


FIG. 1. Direct electron-hole interaction $-W^{\text{in}}$ at $r_s = 22$, in real space (upper panel) and in reciprocal space (bottom), using the static dielectric function from accurate QMC results (black), the RPA (blue), and TCTE calculated using the ALDA kernel (red). In gray $-v_c$, the bare Coulomb interaction. Note that W_{TCTE} is different from the exact W as calculated in QMC and as measurable with classical probes, because it contains the (non-classical) screening contribution felt by a fermion, see main text.

find the well-known high-energy plasmon [4,5,53] with positive quadratic dispersion, which decays into the e - h continuum where $\text{Re } \epsilon^{\text{out}}(q, \omega) \neq 0$ [11,54]. This GW_{RPA} -BSE result resembles the RPA result where self-energy and electron-hole effects are neglected. In both cases the plasmon dispersion is exact at $q \rightarrow 0$ [28]. The e - h interaction in GW_{RPA} -BSE is not strong enough to yield any additional, possibly excitonic, collective mode.

This is not a failure of the RPA e - h screening [28]: the strongly attractive range of the numerically exact W_{QMC} is even shorter than that of W_{RPA} (see Fig. 1). A prominent problem of GW is self-polarization [55–58], since in GW screening happens through variations of the Hartree, but not of the exchange-correlation (xc) potential. The xc variations appear as vertex corrections beyond GW that are important for lower densities [11,26,59–62] and should be considered here. Eliminating the self-polarization weakens the effective screening especially at short range. This is achieved approximately [28] by

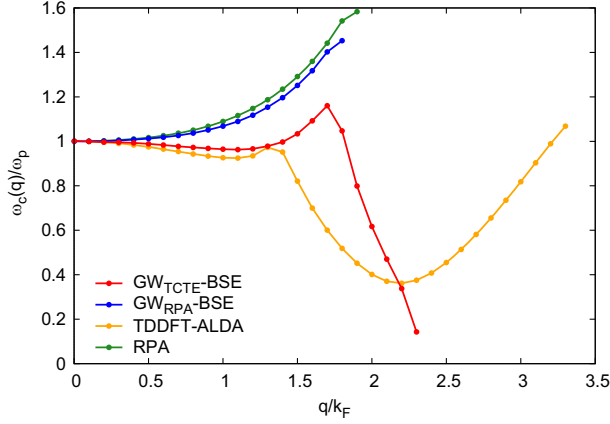


FIG. 2. Collective modes at $r_s = 22$ as a function of wave vector. The lines indicate the solution ω_c of $\text{Re } \epsilon^{\text{out}}(q, \omega_c(q)) = 0$: they stop where no solution is found. In green, RPA result. In orange, TDDFT-ALDA. In blue, $\text{GW}_{\text{RPA-BSE}}$ with $W^{\text{in}} = W_{\text{RPA}}$. In red, $\text{GW}_{\text{TCTE-BSE}}$ with $W^{\text{in}} = W_{\text{TCTE}}$.

using a test-charge-test-electron (TCTE) [31–34,63] inverse dielectric function $1/\epsilon_{\text{in}} = 1 + (v_c + f_{\text{xc}})\chi$ to screen W^{in} , instead of the usual $1/\epsilon_{\text{in}} = 1 + v_c\chi$.

We include the TDDFT xc kernel f_{xc} [35] in the adiabatic local density approximation (ALDA). The bottom panel of Fig. 1 shows $-W_{\text{TCTE}}(q)$. It develops a pronounced dip at $q \sim 2k_F$, in correspondence to a weak feature in $-W_{\text{RPA}}(q)$, and is consistent with the shoulder found in [64] for higher density. In real space, $-W_{\text{TCTE}}(r)$ oscillates at large distances, similarly though more strongly than $-W_{\text{RPA}}(r)$. Most importantly, at short distances r the screened interaction $-W_{\text{TCTE}}(r)$ is closer than $-W_{\text{RPA}}(r)$ to the bare Coulomb interaction $-v_c(r)$, and even stronger than $-v_c(r)$ for $r < 0.5/k_F$. $\text{GW}_{\text{TCTE-BSE}}$ with this enhanced short-range e - h interaction leads to a negative plasmon dispersion, which is an expected xc effect [11,54]. Moreover, the energy of the collective mode decreases abruptly slightly before $q = 2k_F$: the mode drops by more than a factor of 5 up to about $q = 2.4k_F$ evolving into a low-energy mode, before it is damped by other e - h excitations, which makes $\text{Re } \epsilon^{\text{out}}(q, \omega) \neq 0$.

These results agree qualitatively with the prediction of Takada [17,18]. However, benchmarks for spectral features in the low density HEG do not exist. In order to verify the reliability of our findings, we have to resort to static properties, for which accurate QMC benchmarks are available [29]. Indeed, a mode $\text{Re } \epsilon^{\text{out}}(q, \omega_c(q)) = 0$ at low ω_c corresponds to a pole in $\epsilon^{-1}(\omega)$ at low ω , which in turn can cause $\epsilon^{-1}(q, \omega = 0) < 0$ and hence $\epsilon(q, \omega = 0) < 0$. This can only happen when $\epsilon(q, \omega)$ has poles of imaginary energy [15–18]. The negative static screening [11,15–18,54] is therefore an unambiguous fingerprint of these collective modes. It is crucial for the physics of the HEG: this “dielectric catastrophe” regime is the precursor of electronic ground-state

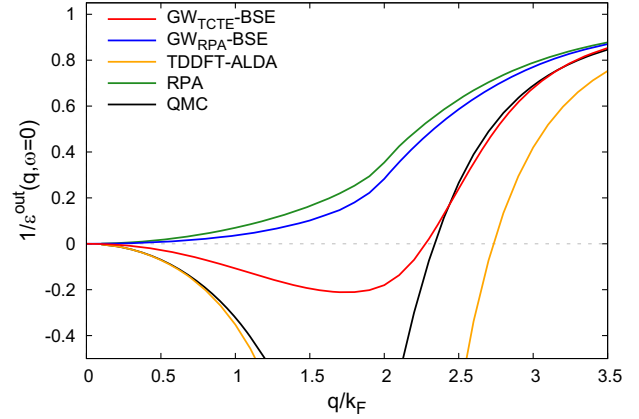


FIG. 3. Static inverse dielectric constant as a function of wave vector for $r_s = 22$. The benchmark (black) is obtained in the interpolation of the QMC data of [29] by Corradini *et al.* [30]. In green, the RPA. In blue, GW-BSE using the RPA W^{in} . In red, GW-BSE using the TCTE W^{in} calculated with the ALDA kernel. In orange, TDDFT in ALDA.

instabilities [15,17,18,54], leading to symmetry breakings such as charge and spin density waves [65]. The static dielectric response delivers therefore key information about possible phase transitions [11,54,66–72].

Figure 3 shows $1/\epsilon^{\text{out}}(q, \omega = 0)$ for $r_s = 22$. The benchmark QMC curve has a minimum around $q = 1.85k_F$, and it is negative up to about $2.35k_F$, where it becomes positive for all larger wave vectors. The $\text{GW}_{\text{TCTE-BSE}}$ result is negative over the same range, although the amplitude is weaker (this is also apparent at smaller r_s [28]), and it follows the exact positive result at larger wave vector. At these large wave vectors the poles of the dielectric function $\epsilon^{\text{out}}(q, \omega)$ at positive real frequencies are twinned by poles at the same absolute, but negative, frequencies. For decreasing wave vector, the two twin poles of $\epsilon^{\text{out}}(q, \omega)$ with, respectively, smallest positive and negative energies move towards each other until they split along the positive and negative imaginary energy axis. This happens when $1/\epsilon^{\text{out}}(q, \omega = 0)$ changes sign. The imaginary poles are called ghost poles [15,16]. These results are in clear contrast to the standard $\text{GW}_{\text{RPA-BSE}}$ results neglecting vertex corrections, which resemble the RPA results where $\epsilon^{\text{out}}(q, \omega = 0)$ never becomes negative (see Fig. 3), consistently with the absence of imaginary poles in $\epsilon^{\text{out}}(q, \omega)$ and with the absence of low-energy modes $\text{Re } \epsilon^{\text{out}}(q, \omega_c(q)) = 0$ in Fig. 2.

The origin of the phenomenon is clearly the e - h attraction: no such mode appears when this interaction is switched off. This speaks for attributing an excitonic origin to both the low-energy mode and the ghost pole. Figure 4 shows for $r_s = 22$ the e - h amplitudes $|\Psi_{\lambda q}(\mathbf{r})|^2$, where $\Psi_{\lambda q}(\mathbf{r})$ are the eigenfunctions of the e - h BSE Hamiltonian. In the HEG they depend only on the e - h distance r and its direction relative to the momentum \mathbf{q} of the excitation.

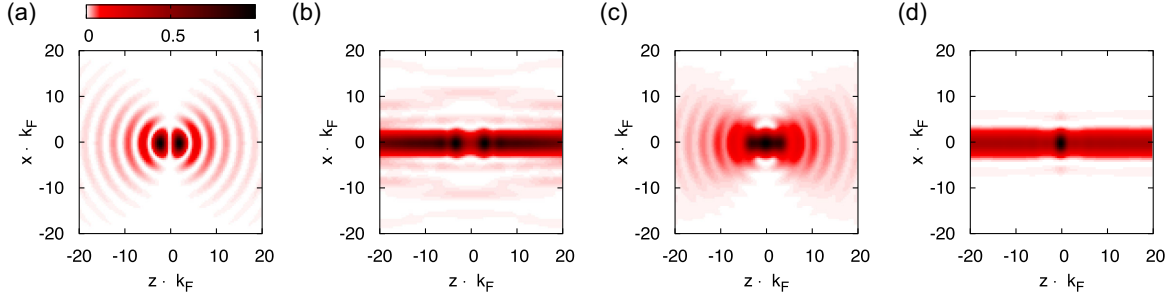


FIG. 4. Absolute square of the correlated e - h amplitude, obtained from (a)–(c) GW_{TCTE} -BSE or (d) TDDFT Casida equation in the ALDA, at $r_s = 22$. Here $\mathbf{q} = q\hat{\mathbf{z}}$. Each e - h amplitude normalised to its maximum value is represented in the xz plane, for $y = 0$. (a) Plasmon at $q = 0.001k_F$. (b) Excitonic collective mode at $q = 2k_F$ from the BSE. (c) Ghost exciton modes obtained for the irreducible polarizability at $q = 0.001k_F$: sum of the two imaginary poles at energies $\pm 5.21i \times 10^{-6}$ Hartree. (d) Excitonic collective mode at $q = 2k_F$ from the TDDFT-ALDA.

For independent electrons and holes this amplitude would be constant, whereas excitonic effects lead to a localization of the electron cloud around the hole [22,73,74].

The excitation λ^q shown in Figs. 4(a)–4(b) is the collective mode represented in Fig. 2. At low q this is the plasmon, for which the e - h amplitude is shown in Fig. 4(a) with \mathbf{q} in the z direction. Its amplitude is different from the RPA result of Egri [75,76], which shows only the resonant part of the amplitude, while here we take all resonant and antiresonant contributions into account. This leads to overall oscillating amplitude and strong cancellations at this small q . Figure 4(b) shows the low-energy collective mode for $q = 2k_F$ at $E_\lambda = 6.627 \times 10^{-3}$ Hartree in GW_{TCTE} -BSE. There is significant localization of the electron around the hole, except for the direction of \mathbf{q} . Figure 4(c) shows the ghost mode for the same small q as the plasmon in Fig. 4(a). Note that here we show the sum of the two imaginary twin ghost poles at energies $\pm i|E|$, while each pole is separately shown in [28]. Interestingly, the shape is quite similar to that of the plasmon. Therefore, a characterization of collective modes according to the shape of the e - h wave function would suggest to speak about a “ghost plasmon” in agreement with the terminology of [15,16], rather than a “ghost exciton” as proposed by Takada [17,18]. The low-energy collective mode in Fig. 4(b), instead, has excitonic character according to the strong two-dimensional localization of the electron around the hole.

The BSE calculations directly display the physics of excitonic effects and suggest pertinent approximations and interpretations, as those above, but they are cumbersome. In principle the dielectric function could also be obtained directly in TDDFT [see alternative to (1) in [28]]. However, two problems arise: first, in semiconductors and insulators long-range effects govern the excitons, for which there are today no efficient and reliable approximations in TDDFT [77]. In the present case, as we have shown above, the physics is dominated by short-range effects, and one may expect that approximations such as the ALDA are

suitable also when used directly in TDDFT. Second, it is less obvious how to analyze the TDDFT results. Similarly to the BSE, one can obtain e - h correlation functions from TDDFT by solving an effective e - h Hamiltonian, which leads to an eigenvalue problem often called the Casida equation [78]. Nevertheless, while exact TDDFT and exact BSE must yield the same dielectric function, we are not aware of any proof that they should also yield the same e - h wave function. However, the BSE and TDDFT Hamiltonians coincide when the effective interaction is ultra short ranged [79].

Figure 2 shows the collective modes obtained in TDDFT-ALDA. At wave vectors around $q = 2k_F$ we do obtain a low-energy mode, in conjunction with the appearance of negative static screening (and therefore, a ghost mode) in Fig. 3. Indeed, the ALDA captures the peculiar features of the low-density HEG, with quantitative agreement at moderate densities and an overestimate of xc effects at very low densities [36,80]. The resulting e - h wave function $|\Psi_{\lambda^q}^{\text{ALDA}}(\mathbf{r})|^2$ is shown in Fig. 4(d) for the excitonic collective mode. It is strikingly similar to the one in Fig. 4(b) resulting from the BSE, although TDDFT and BSE are two completely different approaches. The main difference is that in TDDFT-ALDA the amplitude is more localized. This is consistent with the fact that GW_{TCTE} -BSE underestimates the negative screening, while TDDFT-ALDA has a tendency to overestimate, as shown by Fig. 3. Still, the agreement is surprisingly good, also in view of the simple approximations made here, supporting our understanding in terms of effective short-range interactions.

In conclusion, while simple models [1,2] predict that excitons do not exist in metals due to perfect macroscopic screening, the existence of intriguing phenomena such as low-energy excitonic collective modes, imaginary poles in the dielectric function called ghosts, or negative static screening, are made possible by the imperfect screening of the electron-hole interaction at short distances. This phenomenon can only be captured to a sufficient extent if

xc contributions to the screening are taken into account. This translates into solving the BSE with an effective e - h interaction including vertex corrections beyond those derived from a GW self-energy. Even simple approximations capture the qualitative picture correctly. Dynamical effects that are currently neglected [81] should enhance the effect, reflecting the fact that it takes time to build up a screening cloud [82–84]. The strong dispersion of the low-energy mode, however, suggests significant cancellations of dynamical effects [85], which justifies the static approximation. To get a more precise estimate for dynamical effects and to include vertex corrections beyond TDDFT-derived ones, such as explicit higher order responses from variations of the screening, is a complex task [73,86–89] that is beyond the scope of the present work.

In the low-density HEG, TDDFT in the ALDA also yields pertinent results, but it will break down when long-range effects are important, such as excitons in insulators. The BSE in the form suggested here, instead, is valid over the whole range of length scales. This opens the way for a broad field of potential applications, searching for ghost excitons and the consequent intriguing many-body effects, including the physics of Mott exciton transition and enhanced capacitance linked to negative compressibility [90–95], in systems such as doped or photoexcited semiconductors [96–100], and low-density electron gases at surfaces and interfaces [101–103]. Real materials may be complex, but our predictions based on the HEG are still expected to hold qualitatively, with the challenging exciton physics taking place at short distances.

Acknowledgments—We thank Martin Panholzer and Raymond Frésard for fruitful discussions. This work is supported by a public grant overseen by the French National Research Agency (ANR) as part of the “Investissements d’Avenir” program (Labex NanoSaclay, reference: ANR-10-LABX-0035), by the Magnus Ehrnrooth Foundation, and by the European Research Council (ERC Grant Agreement No. 320971). The research leading to these results has received funding also from the People Programme (Marie Curie Actions) of the European Union’s Seventh Framework Programme (FP7/2007-2013) under REA Grant Agreement No. PCOFUND-GA-2013-609102, through the PRESTIGE programme coordinated by Campus France. Computational time was granted by GENCI (Project No. 544).

-
- [1] R. S. Knox, *Theory of Excitons* (Academic Press, New York, 1963).
 - [2] F. Bassani and G. P. Parravicini, *Electronic States and Optical Transitions in Solids* (Pergamon Press, New York, 1975).
 - [3] F. Bechstedt, *Many-Body Approach to Electronic Excitations: Concepts and Applications*, Springer Series in Solid-State Sciences (Springer, Berlin, Heidelberg, 2014).

- [4] D. Pines and D. Bohm, *Phys. Rev.* **85**, 338 (1952).
- [5] D. Pines, *Elementary Excitations In Solids* (Benjamin, New York, 1963).
- [6] D. M. Ceperley and B. J. Alder, *Phys. Rev. Lett.* **45**, 566 (1980).
- [7] G. Ortiz, M. Harris, and P. Ballone, *Phys. Rev. Lett.* **82**, 5317 (1999).
- [8] F. H. Zong, C. Lin, and D. M. Ceperley, *Phys. Rev. E* **66**, 036703 (2002).
- [9] N. D. Drummond, Z. Radnai, J. R. Trail, M. D. Towler, and R. J. Needs, *Phys. Rev. B* **69**, 085116 (2004).
- [10] M. Holzmann and S. Moroni, *Phys. Rev. Lett.* **124**, 206404 (2020).
- [11] G. Giuliani and G. Vignale, *Quantum Theory of the Electron Liquid* (Cambridge University Press, Cambridge, England, 2005).
- [12] S. Azadi and N. D. Drummond, *Phys. Rev. B* **105**, 245135 (2022).
- [13] Note that negative screening for a range of q does *not* imply necessarily an electronic instability [15] and a globally attractive effective Coulomb interaction. This makes the interpretation of experimental observations, such as the structure factor of expanded liquid alkali metals [14], a non-trivial task.
- [14] K. Matsuda, K. Tamura, and M. Inui, *Phys. Rev. Lett.* **98**, 096401 (2007).
- [15] O. V. Dolgov, D. A. Kirzhnits, and E. G. Maksimov, *Rev. Mod. Phys.* **53**, 81 (1981).
- [16] K. Takayanagi and E. Lipparini, *Phys. Rev. B* **56**, 4872 (1997).
- [17] Y. Takada, *J. Supercond.* **18**, 785 (2005).
- [18] Y. Takada, *Phys. Rev. B* **94**, 245106 (2016).
- [19] W. Schülke, *Electron Dynamics by Inelastic X-Ray Scattering*, Oxford Series on Synchrotron Radiation (Oxford University Press, New York, 2007).
- [20] X. Cui, C. Wang, A. Argondizzo, S. Garrett-Roe, B. Gumhalter, and H. Petek, *Nat. Phys.* **10**, 505 (2014).
- [21] For core electrons, see e.g. G. D. Mahan, *Phys. Rev.* **163**, 612 (1967); P. Nozières and C. T. De Dominicis, *Phys. Rev.* **178**, 1097 (1969).
- [22] R. M. Martin, L. Reining, and D. M. Ceperley, *Interacting Electrons: Theory and Computational Approaches* (Cambridge University Press, Cambridge, England, 2016).
- [23] G. Strinati, *Riv. Nuovo Cim.* **11**, 1 (1988).
- [24] P. Nozières and D. Pines, *Theory Of Quantum Liquids*, (CRC press, Boca Raton, 1999).
- [25] G. D. Mahan, *Many-Particle Physics* (Plenum Press, New York, 1981).
- [26] A. L. Fetter and J. D. Walecka, *Quantum Theory of Many-Particle Systems* (McGraw-Hill, New York, 1971).
- [27] L. Hedin, *Phys. Rev.* **139**, A796 (1965).
- [28] See Supplemental Material at <http://link.aps.org/supplemental/10.1103/PhysRevLett.134.046402> for additional results, which contains Refs. [11,22,25,27,29–45].
- [29] S. Moroni, D. M. Ceperley, and G. Senatore, *Phys. Rev. Lett.* **75**, 689 (1995).
- [30] M. Corradini, R. Del Sole, G. Onida, and M. Palumbo, *Phys. Rev. B* **57**, 14569 (1998).
- [31] P. Streitenberger, *Phys. Lett.* **106A**, 57 (1984).

- [32] G. D. Mahan and B. E. Sernelius, *Phys. Rev. Lett.* **62**, 2718 (1989).
- [33] R. Del Sole, L. Reining, and R. W. Godby, *Phys. Rev. B* **49**, 8024 (1994).
- [34] F. Bruneval, F. Sottile, V. Olevano, R. Del Sole, and L. Reining, *Phys. Rev. Lett.* **94**, 186402 (2005).
- [35] M. Petersilka, U. J. Gossmann, and E. K. U. Gross, *Phys. Rev. Lett.* **76**, 1212 (1996).
- [36] M. Panholzer, M. Gatti, and L. Reining, *Phys. Rev. Lett.* **120**, 166402 (2018).
- [37] M. C. T. D. Müller, C. Friedrich, and S. Blügel, *Phys. Rev. B* **94**, 064433 (2016).
- [38] K. Chen and K. Haule, *Nat. Commun.* **10**, 3725 (2019).
- [39] T. Dornheim, S. Groth, and M. Bonitz, *Phys. Rep.* **744**, 1 (2018).
- [40] T. Dornheim, S. Groth, J. Vorberger, and M. Bonitz, *Phys. Rev. Lett.* **121**, 255001 (2018).
- [41] S. Groth, T. Dornheim, and J. Vorberger, *Phys. Rev. B* **99**, 235122 (2019).
- [42] T. Dornheim, Z. Moldabekov, J. Vorberger, H. Kählert, and M. Bonitz, *Commun. Phys.* **5**, 304 (2022).
- [43] C. A. Kukkonen and K. Chen, *Phys. Rev. B* **104**, 195142 (2021).
- [44] H. M. Böhm, R. Holler, E. Krotscheck, and M. Panholzer, *Phys. Rev. B* **82**, 224505 (2010).
- [45] L. J. Sham and W. Kohn, *Phys. Rev.* **145**, 561 (1966).
- [46] A. Marini and R. Del Sole, *Phys. Rev. Lett.* **91**, 176402 (2003).
- [47] A.-M. Uimonen, G. Stefanucci, Y. Pavlyukh, and R. van Leeuwen, *Phys. Rev. B* **91**, 115104 (2015).
- [48] J. Deslippe, C. D. Spataru, D. Prendergast, and S. G. Louie, *Nano Lett.* **7**, 1626 (2007).
- [49] Y. Liang, R. Soklaski, S. Huang, M. W. Graham, R. Havener, J. Park, and L. Yang, *Phys. Rev. B* **90**, 115418 (2014).
- [50] E. Maggio and G. Kresse, *Phys. Rev. B* **93**, 235113 (2016).
- [51] J. Friedel, *Lond. Edinb. Dubl. Phil. Mag.* **43**, 153 (1952).
- [52] W. Harrison, *Solid State Theory*, Dover Books on Physics (Dover Publications, New York, 1980).
- [53] K. Sawada, K. A. Brueckner, N. Fukuda, and R. Brout, *Phys. Rev.* **108**, 507 (1957).
- [54] S. Ichimaru, *Rev. Mod. Phys.* **54**, 1017 (1982).
- [55] W. Nelson, P. Bokes, P. Rinke, and R. W. Godby, *Phys. Rev. A* **75**, 032505 (2007).
- [56] P. Romaniello, S. Guyot, and L. Reining, *J. Chem. Phys.* **131**, 154111 (2009).
- [57] F. Aryasetiawan, R. Sakuma, and K. Karlsson, *Phys. Rev. B* **85**, 035106 (2012).
- [58] Y.-W. Chang and B.-Y. Jin, *Phys. Scr.* **86**, 065301 (2012).
- [59] H. Yasuhara, *J. Phys. Soc. Jpn.* **36**, 361 (1974).
- [60] R. Mattuck, *A Guide to Feynman Diagrams in the Many-body Problem*, Dover Books on Physics Series (Dover Publications, New York, 1992).
- [61] A. Imler, A. Gallo, F. Hummel, and A. Grüneis, *Phys. Rev. Lett.* **123**, 156401 (2019).
- [62] K. S. Singwi, M. P. Tosi, R. H. Land, and A. Sjölander, *Phys. Rev.* **176**, 589 (1968).
- [63] M. S. Hybertsen and S. G. Louie, *Phys. Rev. B* **35**, 5585 (1987).
- [64] C. F. Richardson and N. W. Ashcroft, *Phys. Rev. B* **50**, 8170 (1994).
- [65] A. W. Overhauser, *Phys. Rev.* **167**, 691 (1968).
- [66] D. Thouless, *The Quantum Mechanics of Many-body Systems* (Academic Press, New York, 1972).
- [67] K. Sawada and N. Fukuda, *Prog. Theor. Phys.* **25**, 653 (1961).
- [68] H. B. Shore, E. Zaremba, J. H. Rose, and L. Sander, *Phys. Rev. B* **18**, 6506 (1978).
- [69] L. M. Sander, J. H. Rose, and H. B. Shore, *Phys. Rev. B* **21**, 2739 (1980).
- [70] H. Iyetomi, K. Utsumi, and S. Ichimaru, *Phys. Rev. B* **24**, 3226 (1981).
- [71] J. P. Perdew and T. Datta, *Phys. Status Solidi (b)* **102**, 283 (1980).
- [72] J. P. Perdew, A. Ruzsinszky, J. Sun, N. K. Nepal, and A. D. Kaplan, *Proc. Natl. Acad. Sci. U.S.A.* **118**, e2017850118 (2021).
- [73] M. Rohlfing and S. G. Louie, *Phys. Rev. B* **62**, 4927 (2000).
- [74] The BSE in the singlet channel gives collective exciton modes, while the triplet gives ghost modes.
- [75] I. Egri, *Z. Phys. B Condensed Matter* **53**, 183 (1983).
- [76] I. Egri, *Phys. Rep.* **119**, 363 (1985).
- [77] S. Botti, A. Schindlmayr, R. D. Sole, and L. Reining, *Rep. Prog. Phys.* **70**, 357 (2007).
- [78] M. E. Casida, Time-dependent density functional response theory for molecules, in *Recent Advances in Density Functional Methods*, edited by D. P. Chong (World Scientific, Singapore, 1995), pp. 155–192.
- [79] G. Onida, L. Reining, and A. Rubio, *Rev. Mod. Phys.* **74**, 601 (2002).
- [80] A. D. Kaplan, N. K. Nepal, A. Ruzsinszky, P. Ballone, and J. P. Perdew, *Phys. Rev. B* **105**, 035123 (2022).
- [81] G. Strinati, *Phys. Rev. Lett.* **49**, 1519 (1982).
- [82] G. S. Canright, *Phys. Rev. B* **38**, 1647 (1988).
- [83] M. Alducin, J. I. Juaristi, and P. M. Echenique, *Surf. Sci.* **559**, 233 (2004).
- [84] W.-D. Schöne and W. Ekardt, *Phys. Rev. B* **62**, 13464 (2000).
- [85] P. Cudazzo and L. Reining, *Phys. Rev. Res.* **2**, 012032(R) (2020).
- [86] Y. Ma, M. Rohlfing, and C. Molteni, *Phys. Rev. B* **80**, 241405(R) (2009).
- [87] C. D. Spataru and F. Léonard, *Chem. Phys.* **413**, 81 (2013).
- [88] S. Gao, Y. Liang, C. D. Spataru, and L. Yang, *Nano Lett.* **16**, 5568 (2016).
- [89] P.-F. Loos and X. Blase, *J. Chem. Phys.* **153**, 114120 (2020).
- [90] J. P. Eisenstein, L. N. Pfeiffer, and K. W. West, *Phys. Rev. Lett.* **68**, 674 (1992).
- [91] L. Li, C. Richter, S. Paetel, T. Kopp, J. Mannhart, and R. C. Ashoori, *Science* **332**, 825 (2011).
- [92] V. Tinkl, M. Breitschaft, C. Richter, and J. Mannhart, *Phys. Rev. B* **86**, 075116 (2012).
- [93] R. Frésard, K. Steffen, and T. Kopp, *Phys. Rev. B* **105**, 245118 (2022).
- [94] J. He *et al.*, *Nat. Mater.* **14**, 577 (2015).
- [95] J. M. Riley, W. Meevasana, L. Bawden, M. Asakawa, T. Takayama, T. Eknepakul, T. K. Kim, M. Hoesch,

- S.-K. Mo, H. Takagi, T. Sasagawa, M. S. Bahramy, and P. D. C. King, *Nat. Nanotechnol.* **10**, 1043 (2015).
- [96] N. F. Mott, *Rev. Mod. Phys.* **40**, 677 (1968).
- [97] J. Shah, M. Combescot, and A. H. Dayem, *Phys. Rev. Lett.* **38**, 1497 (1977).
- [98] A. Schleife, C. Rödl, F. Fuchs, K. Hannewald, and F. Bechstedt, *Phys. Rev. Lett.* **107**, 236405 (2011).
- [99] A. Steinhoff, M. Florian, M. Rösner, G. Schönhoff, T. O. Wehling, and F. Jahnke, *Nat. Commun.* **8**, 1166 (2017).
- [100] T. Siday, F. Sandner, S. Brem, M. Zizlsperger, R. Perea-Causin, F. Schiegl, S. Nerreter, M. Plankl, P. Merkl, F. Mooshammer, M. A. Huber, E. Malic, and R. Huber, *Nano Lett.* **22**, 2561 (2022).
- [101] A. Ohtomo and H. Y. Hwang, *Nature (London)* **427**, 423 (2004).
- [102] A. F. Santander-Syro, O. Copie, T. Kondo, F. Fortuna, S. Pailhès, R. Weht, X. G. Qiu, F. Bertran, A. Nicolaou, A. Taleb-Ibrahimi, P. Le Fèvre, G. Herranz, M. Bibes, N. Reyren, Y. Apertet, P. Lecoeur, A. Barthélémy, and M. J. Rozenberg, *Nature (London)* **469**, 189 (2011).
- [103] X. Lin, Z. Zhu, B. Fauqué, and K. Behnia, *Phys. Rev. X* **3**, 021002 (2013).